Electronic Supplementary Information

A Highly Selective Fluorescence Turn–On Chemosensor for Zn^{2+}, its Application in Live Cell Imaging, and a Colorimetric Sensor for Co^{2+}: Experimental and TD-DFT Calculations

Marzieh Sohrabi,[a] Mehdi Amirnasr,[a,*] Soraia Meghdadi,[a,*] Martin Lutz,[b] Maryam Bikhof Torbati,[c] Hossein Farrokhpour [a]

[a] *Department of Chemistry, Isfahan University of Technology, Isfahan 8415683111, Iran*

[b] *Crystal and Structural Chemistry, Bijvoet Center for Biomolecular Research, Faculty of Science, Utrecht University, Padualaan 8, 3584 CH Utrecht, The Netherlands*

[c] *Department of Biology, College of Basic Science, Shahr-e-Rey Branch, Islamic Azad University, Tehran 1815163111, Iran*

Synthesis of carboxamide ligand, Hbpq

A mixture of triphenylphosphite (TPP) (5 mmol, 1.55 g), tetrabutylammonium bromide (TBAB) (5 mmol, 1.61 g), pyridine-2-carboxcilic acid (5 mmol, 0.62 g), and 8-aminoquinoline (5 mmol, 0.72 g) in a 25-mL round bottom flask was placed in an oil bath. The reaction mixture was heated until a homogeneous solution was formed, and the solution was stirred for 30 min at 120 °C. The final viscous solution was cooled to room temperature and then treated with 10 mL of cold ethanol. The product was precipitated out and filtered off and washed with cold ethanol.

Yield 84%. Anal. Calcd. for $C_{15}H_{11}N_3O$: C, 72.28; H, 4.45; N, 16.86. Found: C, 72.18; H, 4.27; N, 16.76%. FT–IR (KBr, cm^{-1}) υ_{max}: 3295 (s, N-H), 1681 (s, C=O), 1529 (m, C=C), 1487 (m, C–N). UV–Vis: [CH_3CN; λ_{max} (nm) (ε, L mol^{-1} cm^{-1})]: 328 (12240), 276 (7510), 241 (23950). ^1H NMR (δ, $CDCl_3$, 500 MHz): 7.45-7.63 (m, 4H, $H_{b,d,e,i}$) 7.91 (td, H_h), 8.18 (dd, H_c), 8.35 (bd, H_g), 8.78 (bd, H_f), 8.96 (dd, H_j), 9.01 (dd, H_a), 12.27 (s, NH).

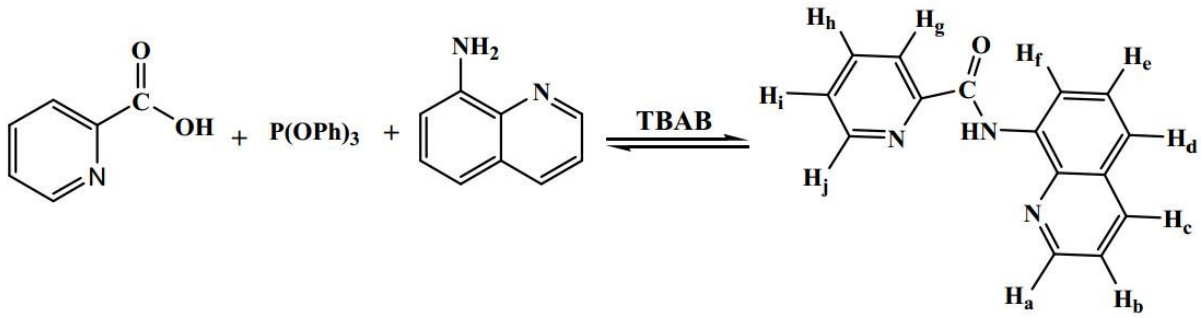

Scheme S1. One pot synthesis of N-(8-quinolyl)pyridine-2-carboxamide ligand, Hbpq.

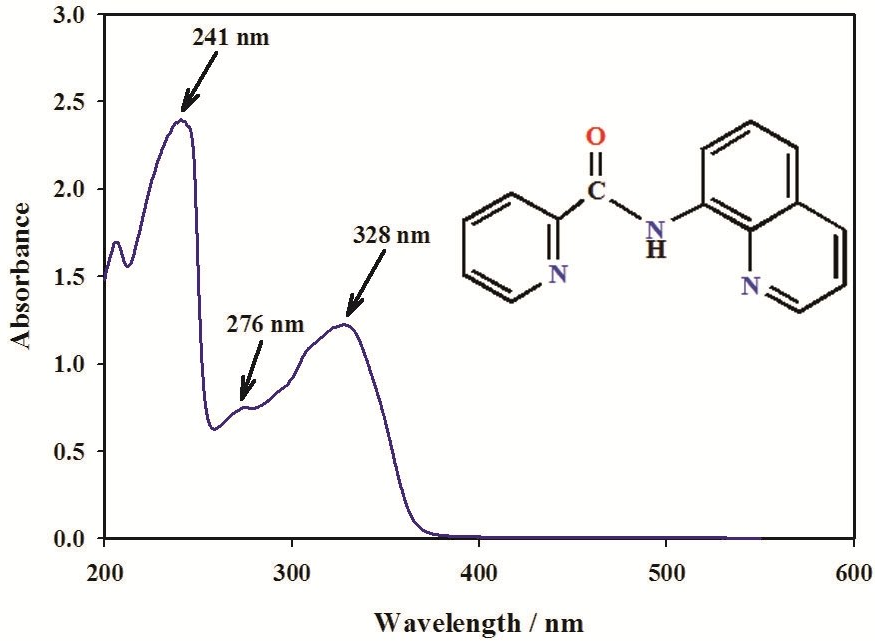

Fig. S1-1. UV-vis spectrum of Hbpq in acetonitrile, solution at room temperature.

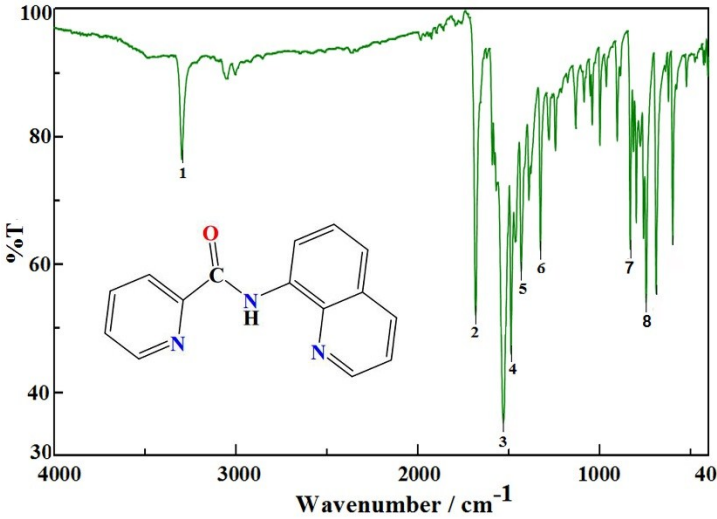

Result of Peak Picking		
No.	**cm^{-1}**	**%T**
1	3295.75	76.5090
2	1681.62	52.0919
3	1529.27	35.4457
4	1486.85	45.9958
5	1430.92	58.9611
6	1324.86	62.2769
7	832.13	62.4270
8	743.42	54.0792

Fig. S1-2. FT-IR spectrum of Hbpq (KBr pellet).

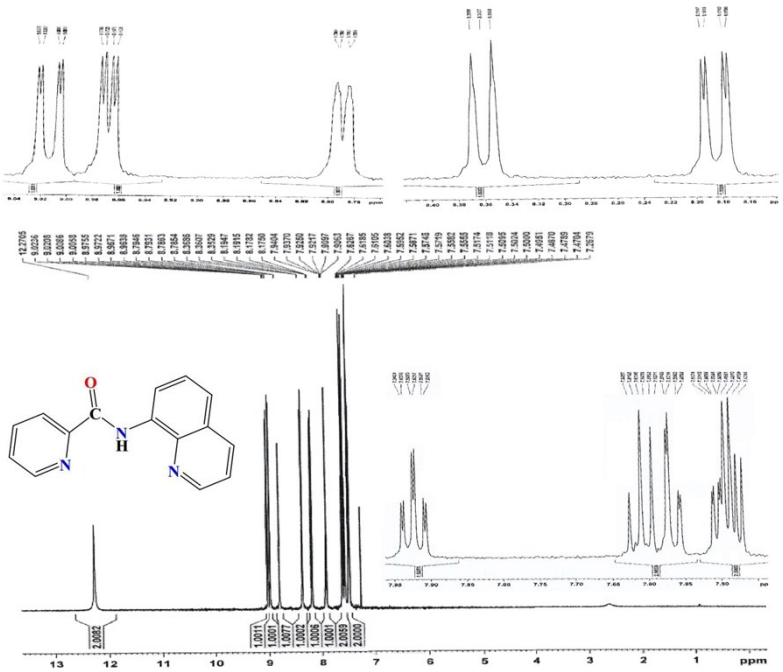

Fig. S1-3. ^{1}H NMR spectrum of Hbpq in $CDCl_3$, solution at room temperature.

Determination of association constant for Zn^{2+} complex

An association constant (2:1) was calculated according to the titration curve for complex formation between the chemosensors and the metal ions, using the following nonlinear least squares fitting equation:

$$y = \frac{x}{2 \times a \times b \times (1-x)^2} + \frac{x \times b}{2}$$

Where ***a*** is the association constant, ***b*** is the concentration of chemosensor, ***x*** is A_x-A_0/A_{max}-A_0 and ***y*** is the concentration of metal ions [1].

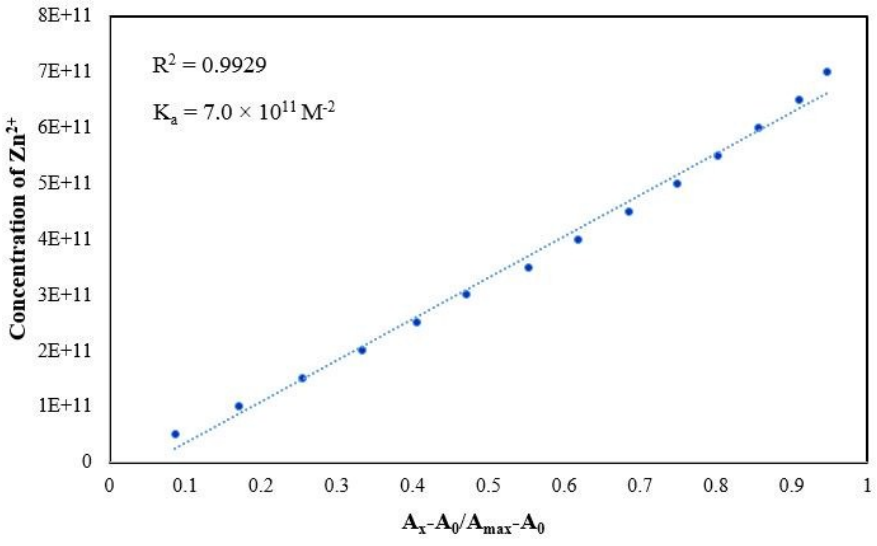

Fig. S2. The Benesi-Hildebrand plot of Hbpq with Zn^{2+} based on the absorption titration.

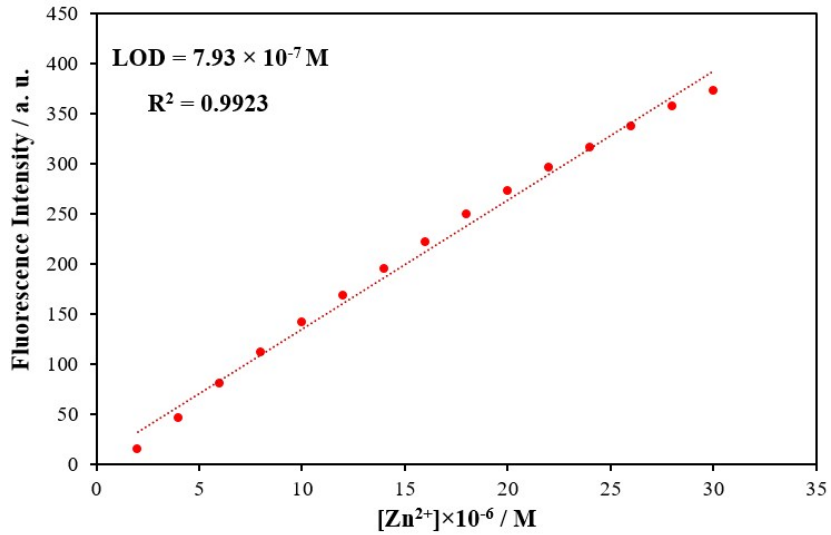

Fig. S3. The linear fitting of the fluorescence intensity of Hbpq toward the concentrations of Zn^{2+}.

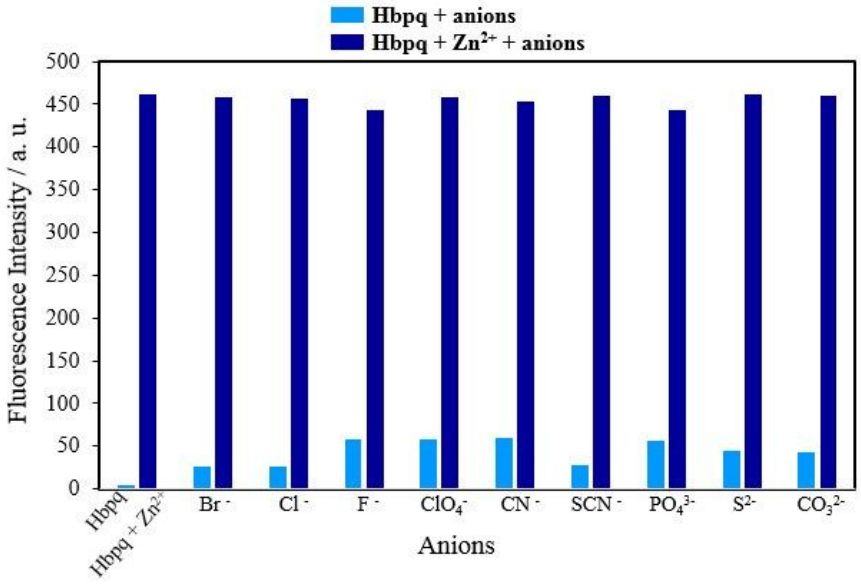

Fig. S4. The relative fluorescence intensity of Hbpq and $[Zn(bpq)_2]$ in the presence of interfering anions.

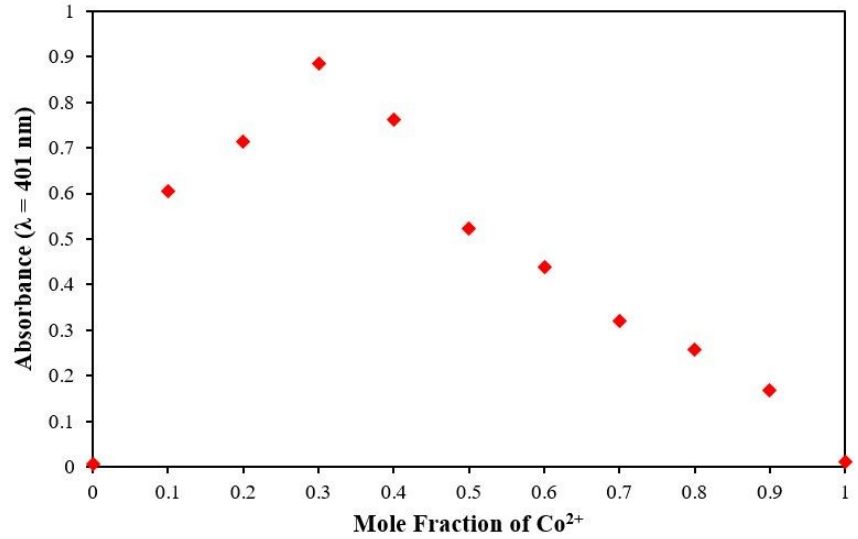

Fig. S5. Job's plot of the $[Co(bpq)_2]$ complex in acetonitrile solution, with the monitoring wavelength set at 401 nm.

Determination of association constant for Co^{2+} complex

An association constant (2:1) was calculated according to the titration curve for complex formation between the chemosensors and the metal ions, using the following nonlinear least squares fitting equation:

$$y = \frac{x}{2 \times a \times b \times (1-x)^2} + \frac{x \times b}{2}$$

Where ***a*** is the association constant, ***b*** is the concentration of chemosensor, ***x*** is A_x-A_0/A_{max}-A_0 and ***y*** is the concentration of metal ions [1].

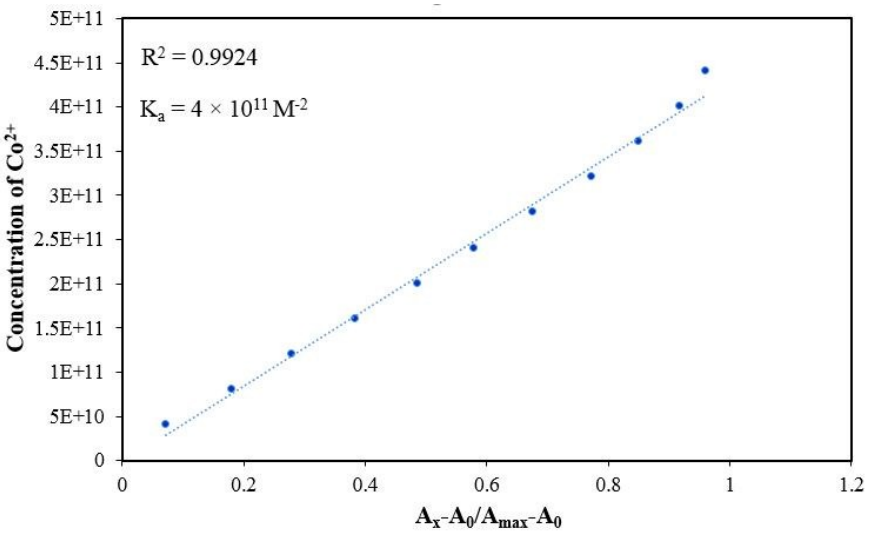

Fig. S6. The Benesi-Hildebrand plot of Hbpq with Co^{2+} based on the absorption titration.

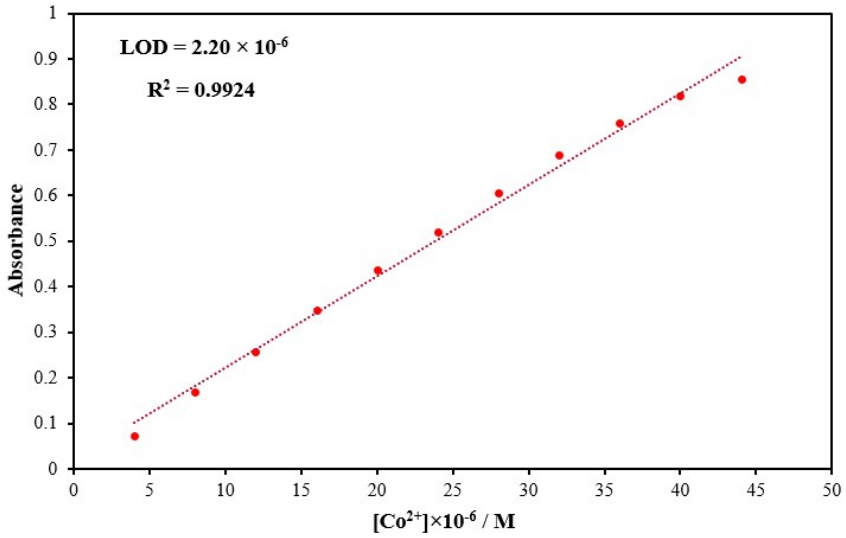

Fig. S7. The linear fitting of the absorption intensity of Hbpq toward the concentrations of Co^{2+}.

Reference

1 L. Neupane, J. Park, J. Park, and K. Lee, *org. lett.*, 2013, **15**, 254.

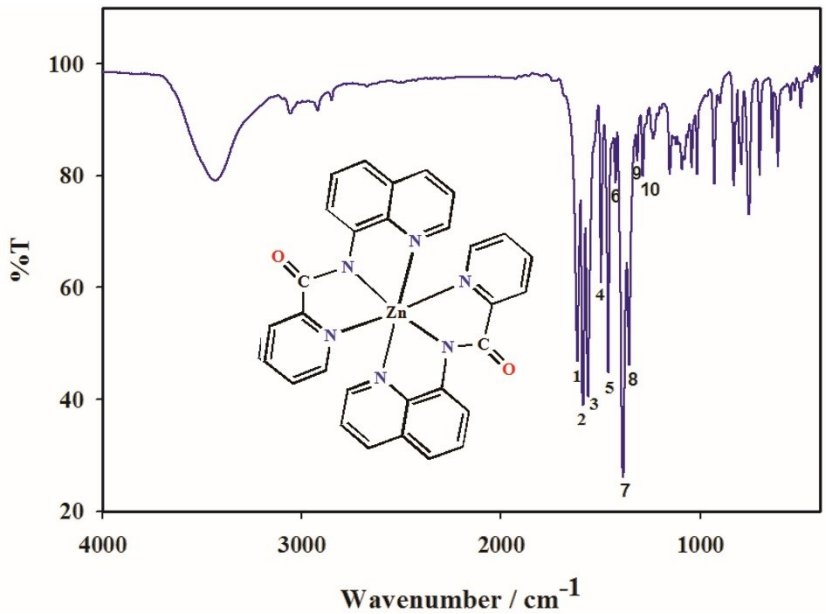

Result of Peak Picking		
No.	**cm^{-1}**	**%T**
1	1616.06	46.7841
2	1589.06	39.0513
3	1562.06	40.5179
4	1497.45	61.0136
5	1460.81	44.7353
6	1424.17	78.7334
7	1386.57	26.1374
8	1356.68	46.1951
9	1315.21	82.6825
10	1287.25	80.0554

Fig. S8. FT-IR spectrum of $[Zn(Hbpq)_2]$ as KBr pellet.

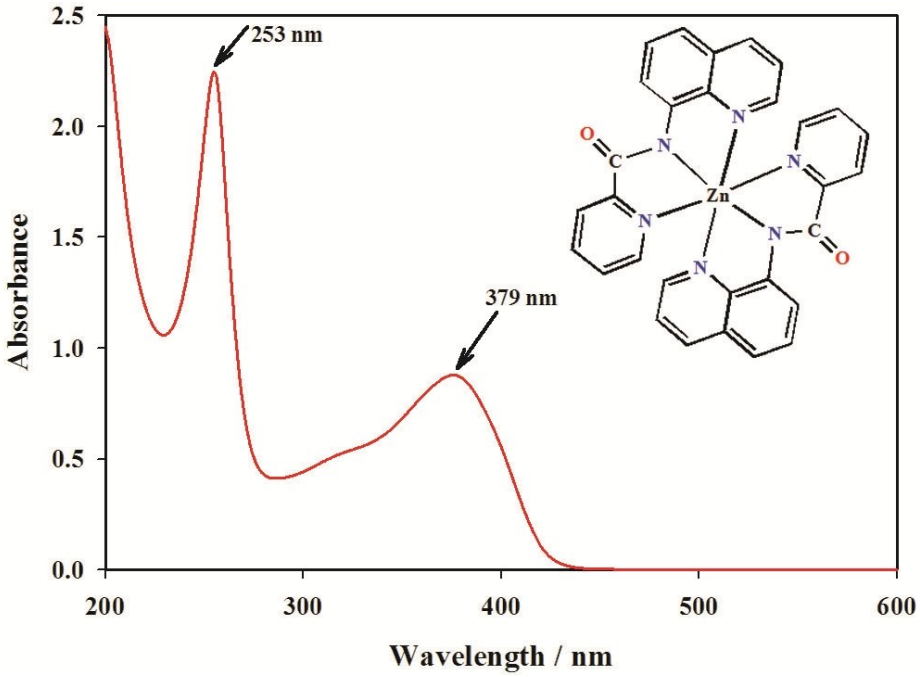

Fig. S9. UV-vis spectrum of $[Zn(bpq)_2]$ in acetonitrile, solution at room temperature.

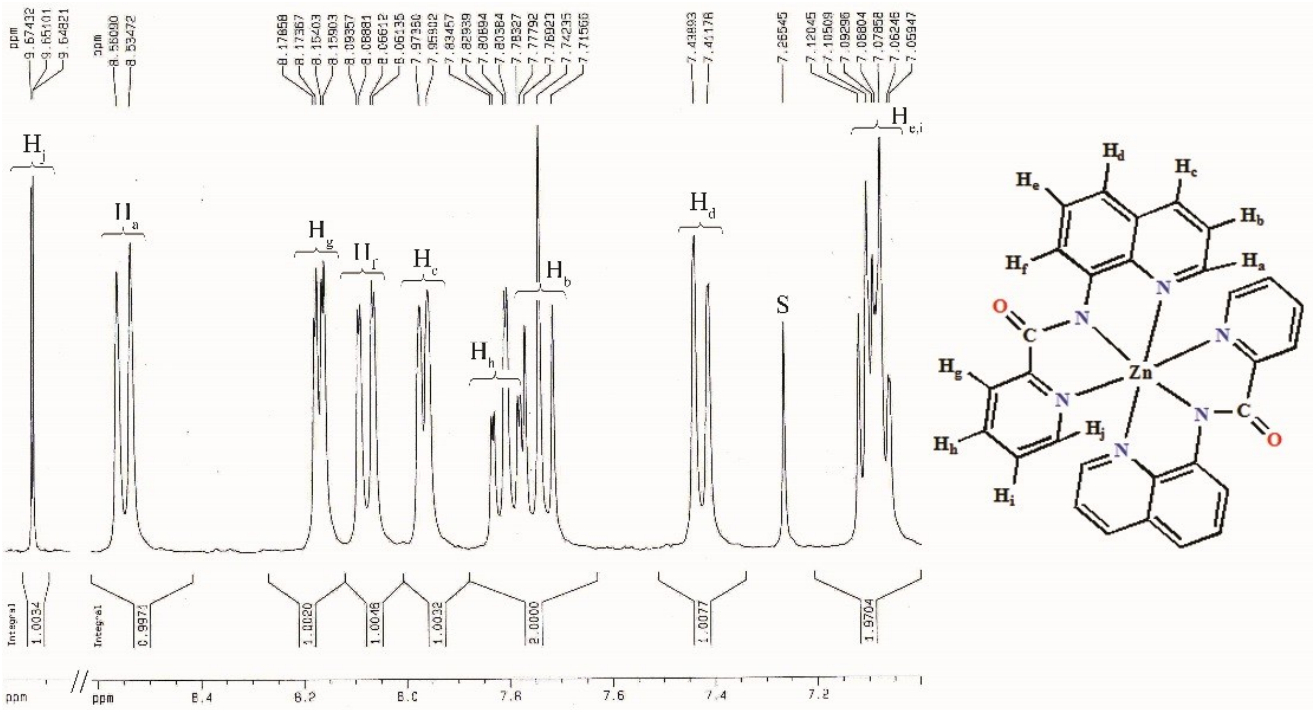

Fig. S10. ^{1}H-NMR spectrum of $[Zn(Hbpq)_2]$ in $CDCl_3$ solution at room temperature.

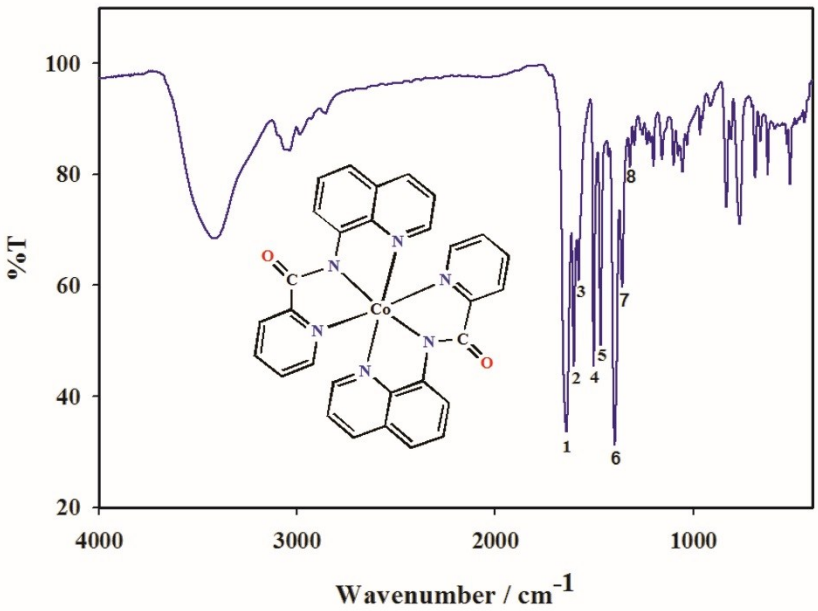

Result of Peak Picking		
No.	**cm^{-1}**	**%T**
1	1639.20	33.6528
2	1602.56	45.5338
3	1577.49	60.9859
4	1502.28	45.5313
5	1466.60	49.1888
6	1396.21	31.2252
7	1357.64	59.7243
8	1319.07	81.2741

Fig. S11. FT-IR spectrum of [Co(Hbpq)$_2$] as KBr pellet.

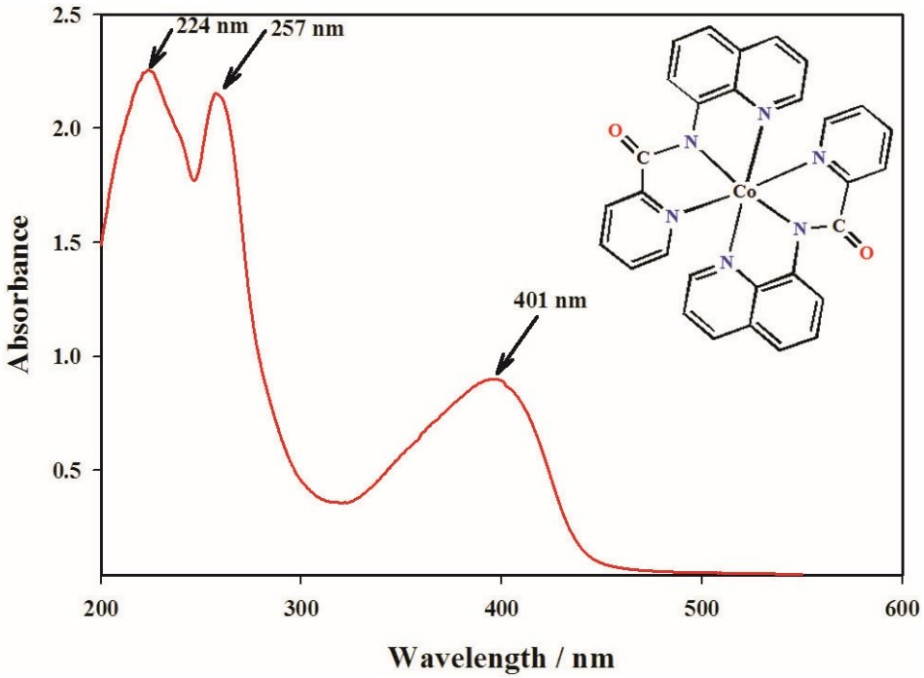

Fig. S12. UV-vis spectrum of [Co(bpq)$_2$] in acetonitrile, solution at room temperature.